

# Lawrence Berkeley National Laboratory

## Recent Work

### Title

ISOSPIN-FORBIDDEN DECAY PROPERTIES OF THE LOWEST  $T = 2$  STATES OF  $^{20}\text{Ne}$ ,  $^{24}\text{Mg}$ ,  $^{28}\text{Si}$ ,  $^{32}\text{S}$ , AND  $^{40}\text{Ca}$

### Permalink

<https://escholarship.org/uc/item/8jc7446d>

### Authors

McGrath, Robert L.

Cerny, Joseph

Hardy, J.C.

et al.

### Publication Date

1969-06-01

Submitted to Physical Review

UCRL-18940  
Preprint

*cy. Z*

ENR. DIV. LIBRARY

JUL 29 1969

LIBRARY AND  
DOCUMENTS SECTION

ISOSPIN-FORBIDDEN DECAY PROPERTIES OF THE LOWEST  
T = 2 STATES OF  $^{20}\text{Ne}$ ,  $^{24}\text{Mg}$ ,  $^{28}\text{Si}$ ,  $^{32}\text{S}$ , AND  $^{40}\text{Ca}$

Robert L. McGrath, Joseph Cerny, J. C. Hardy,  
G. Goth and Akito Arima

June 1969

AEC Contract No. W-7405-eng-48

TWO-WEEK LOAN COPY

This is a Library Circulating Copy  
which may be borrowed for two weeks.  
For a personal retention copy, call  
Tech. Info. Division, Ext. 5545

LAWRENCE RADIATION LABORATORY  
UNIVERSITY of CALIFORNIA BERKELEY

UCRL-18940

## **DISCLAIMER**

This document was prepared as an account of work sponsored by the United States Government. While this document is believed to contain correct information, neither the United States Government nor any agency thereof, nor the Regents of the University of California, nor any of their employees, makes any warranty, express or implied, or assumes any legal responsibility for the accuracy, completeness, or usefulness of any information, apparatus, product, or process disclosed, or represents that its use would not infringe privately owned rights. Reference herein to any specific commercial product, process, or service by its trade name, trademark, manufacturer, or otherwise, does not necessarily constitute or imply its endorsement, recommendation, or favoring by the United States Government or any agency thereof, or the Regents of the University of California. The views and opinions of authors expressed herein do not necessarily state or reflect those of the United States Government or any agency thereof or the Regents of the University of California.

ISOSPIN-FORBIDDEN DECAY PROPERTIES OF THE LOWEST  $T = 2$  STATES OF  
 $^{20}\text{Ne}$ ,  $^{24}\text{Mg}$ ,  $^{28}\text{Si}$ ,  $^{32}\text{S}$ , AND  $^{40}\text{Ca}^\dagger$

Robert L. McGrath

Department of Physics, State University of New York  
Stony Brook, New York 11790

Joseph Cerny, J. C. Hardy, and G. Goth

Department of Chemistry and Lawrence Radiation Laboratory  
University of California, Berkeley, California 94720

and

Akito Arima

Department of Physics, University of Tokyo  
Tokyo, Japan

June 1969

ABSTRACT

The lowest  $T = 2$  states of  $^{20}\text{Ne}$ ,  $^{24}\text{Mg}$ ,  $^{28}\text{Si}$ ,  $^{32}\text{S}$ , and  $^{40}\text{Ca}$  have been formed using the (p,t) reaction. The isospin-forbidden proton ( $\Delta T = 1$  or 2) and alpha particle ( $\Delta T = 2$ ) decay modes of these states have been determined by counting triton-proton and triton-alpha coincidence events. The major decay modes of the states are:  $^{20}\text{Ne}(\alpha_1 + \alpha_2, \alpha_3 + \alpha_4)$ ;  $^{24}\text{Mg}(p_0)$ ;  $^{28}\text{Si}(\alpha_0)$ ;  $^{32}\text{S}(p_0)$ ;  $^{40}\text{Ca}(\alpha_0)$ . Simple Coulomb calculations were performed for  $^{40}\text{Ca}$ ; these assumed pure shell-model configurations and considered isospin mixing in only the (1d,1f) shells. They did not predict the relatively large  $\Delta T = 2$  isospin impurities necessary to explain the observed alpha-particle decay.

## INTRODUCTION

It is well known that isobaric analog states in light and heavy nuclides can be characterized to a good approximation by a single isospin quantum number since the nuclear force is nearly charge-independent. The magnitudes of  $\Delta T = 1$  impurities introduced by the Coulomb potential in low-lying states of several  $T = 0$  light nuclides have been calculated by MacDonald<sup>1</sup> and found to be small. From experimental data on isospin-forbidden gamma and particle transitions, Wilkinson<sup>2</sup> observed that the impurities were in substantial agreement with these theoretical estimates. Blin-Stoyle<sup>3</sup> has summarized analyses of both beta-decay rates and masses of the mass-14  $T = 1$  states in terms of the Coulomb potential plus a generalized charge-dependent nuclear force. He concludes that "none of the data are inconsistent with a nuclear charge-dependent force of the order of a percent or so." One hopes that studies of "isospin-forbidden" processes may provide information about the form of nuclear charge-dependent interactions in nuclei, or at least, about the wave functions admixed by these interactions.

In this paper, experimental data on the isospin-forbidden particle decay of five  $T = 2$  analog states in self-conjugate  $T_z = (N-Z)/2 = 0$  nuclides are presented. The  $T = 2$  states are analogs of the ground state of the  $(Z-2, N+2)$  nuclides with spin-parity  $0^+$  and are readily formed in two-nucleon transfer reactions on  $T = 1$  target nuclides. Several of these states also have been observed<sup>4,5,6</sup> as isospin-forbidden compound nucleus resonances having total widths less than 2.5 keV, the small widths presumably reflecting a relatively high degree of isospin purity since none of the states have any isospin-allowed particle decay modes. A comprehensive review of experimental data on analog states, containing literature references on  $T = 2$  states, has been given recently.<sup>7</sup>



## EXPERIMENTAL PROCEDURE

The data were obtained using proton beams from the Berkeley 88-inch cyclotron. The beam energy was adjusted from 42 MeV to 46 MeV, depending on the Q-values for formation of the  $T = 2$  states, in order that outgoing tritons in the forward direction had energies of approximately 20 MeV. Previous work had indicated that the (p,t) cross sections are maximized around this energy.<sup>11</sup>

Self-supporting targets of  $^{26}\text{Mg}$  (99.2% enriched),  $^{30}\text{Si}$  (89%),  $\text{Cd}^{34}\text{S}$  (37.2%), and  $^{42}\text{Ca}$  (94.4%) were used. The  $^{26}\text{Mg}$  target was about  $1 \text{ mg/cm}^2$  thick, and the others were between 400 and  $500 \mu\text{g/cm}^2$  thick. The  $^{20}\text{Ne}$  data were collected using a  $^{22}\text{Ne}$  gas target and the experimental arrangement will be discussed separately. Outgoing tritons were detected in a counter telescope positioned at +22 degrees with respect to the beam direction; this angle is at the second maximum of the  $L = 0$  angular distributions to the analog states. The (p,t) cross sections at this angle are only about 80 to  $100 \mu\text{b/sr}$ ; therefore, two "decay" counter telescopes were operated in parallel in order to increase the data acquisition rate. These two telescopes were fixed at -90 degrees and -125 degrees. All three telescopes consisted of  $\Delta E$ , E, and E-reject silicon-semiconductor detectors (the last being used to reject particles that passed through the E detector). Each of the "decay" telescopes consisted of  $50\mu$   $\Delta E$ ,  $280\mu$  E, and  $500\mu$  E-reject detectors. Decay alpha particles from the analog states could not penetrate the  $\Delta E$  detectors, but could be identified unambiguously from the reaction kinematics. A schematic representation of the experimental apparatus is shown in Fig. 1.

Signals from each detector were amplified and passed on to Goulding-Landis particle identifiers. Triton singles energy spectra were accumulated

in the memory core of an on-line PDP-5 computer using a multiplexer and analog-to-digital converter. If pulses occurred in either of the decay  $\Delta E$  detectors in fast coincidence ( $2\tau \sim 50$  ns) with a pulse in the triton  $\Delta E$  detector, then the appropriate telescope signals were fed to the particle identifiers. Provided the event involved a triton in the triton telescope and either a proton or a particle stopping in the  $\Delta E$  detector of either decay telescope, total energy signals together with the necessary logic signals were passed on to the computer and the data were stored on magnetic tape for later analysis. These data were finally displayed and plotted as  $512 \times 512$  channel two-dimensional energy spectra together with the 512 channel triton singles data.

Apertures placed in front of the detectors served to define the acceptance solid angles; additional apertures and magnets placed in front of the defining apertures helped to reduce the electron noise background. The triton telescope subtended  $9.2 \times 10^{-4}$  sr. The  $\Delta E$  detectors of the decay telescopes subtended about  $1.5 \times 10^{-2}$  sr and the E detectors subtended about  $1.2 \times 10^{-2}$  sr. These relatively large solid angles, necessary to insure reasonable data accumulation rates, were obtained by using detectors about 1.2 cm in diameter as well as 1 cm defining apertures. Since the calculated branching ratios depend on the solid angles of the decay telescopes, and "dead" regions near the edge of the depleted volumes of the detectors might have reduced the effective solid angles, compared to those found from geometrical measurements, two methods were employed to measure these angles by actual particle counting. First the  $\Delta E$  solid angles were determined to  $\pm 5\%$  by mounting a  $^{212}\text{Pb}$  alpha-particle source in the target plane (masked by an aperture the size of typical proton beam spots) and comparing the  $\Delta E$  counting rates to those of a detector



placed behind a much smaller aperture of known solid angle. The E solid angles were found to  $\pm 15\%$  using data from the  $^{19}\text{F}(p,t)^{17}\text{F}$  (3.10 MeV)  $\rightarrow$  p +  $^{16}\text{O}$  reaction. The  $^{17}\text{F}$  3.10 MeV state with spin 1/2 decays 100 percent by isotropic proton emission (in the  $^{17}\text{F}$  recoil coordinate system) to the  $^{16}\text{O}$  ground state. A 36 MeV proton beam and a  $\text{CaF}_2$  target were used to obtain the triton-proton decay coincidence data. These data were then analyzed in the manner described below, to yield the E detector solid angles.

A single decay telescope consisting of a  $37\mu$   $\Delta\text{E}$  and  $275\mu$  E detector was used in the  $^{20}\text{Ne}$  experiment. The 6.4 cm diam cylindrical  $^{22}\text{Ne}$  (91.3%) gas target was covered with  $25\mu$  Havar foil; a tube at  $-90$  degrees projected into the target volume so that a  $6.4\mu$  Mylar foil window could be mounted 1.25 cm from the reaction volume. The reaction volume was defined by two apertures placed in front of the triton telescope positioned at  $+22.8$  degrees. The decay telescope at  $-90$  degrees viewed the entire reaction volume through the Mylar window; this thin window allowed relatively low energy decay products to escape the target with only minor energy losses or straggling. The decay telescope geometry guaranteed equally efficient detection of decay particles which originated anywhere in the reaction volume. The solid angle of the decay telescope was defined by a single aperture in front of the  $\Delta\text{E}$  detector and was calculated from the geometry to be  $6.0 \times 10^{-3}$  sr ( $\pm 20\%$ ).

## DATA ANALYSIS

Coincidence data from the  $^{42}\text{Ca}(p,t)^{40}\text{Ca}$  reactions are exhibited as two-dimensional energy spectra in Figs. 2 and 3 and are typical. The kinematics of reactions with three-particle final states are completely specified if the momenta of two of the particles are measured. Thus, the data are expected to lie along bands determined by the kinematics and experimental resolution. The diagonal lines shown in the figures were calculated from the kinematics and many events cluster along the  $^{39}\text{K}(\text{g.s.}) + p$  and  $^{36}\text{Ar}(\text{g.s.}) + \alpha$  lines. Typically, the overall triton resolution was 130 keV and the proton resolution was about 100 keV. The overall alpha particle ( $\Delta E$ ) resolution was primarily determined by energy losses in the target. The events in the figures corresponding to 24.8 MeV tritons are accidentals associated with the high yield  $^{16}\text{O}(p,t)^{14}\text{O}$  contaminant reaction; the number of these events was used as a measure of the chance-coincidence rate.

Data along the kinematic lines were added from both decay telescopes and projected onto the triton energy axis in order to find the decay properties of the  $T = 2$  states. Figure 4 shows these projections of the  $^{40}\text{Ca}$  data along with the triton singles energy spectrum. The triton spectrum cuts off at about 26 MeV because of the relatively thin triton telescope detectors which were employed in order to lower the chance coincidence rates. The largest peak in the singles spectrum, excepting contaminants, corresponds to the  $^{40}\text{Ca} T = 2$  state at  $11.978 \pm 0.025$  MeV. The  $^{36}\text{Ar}(\text{g.s.}) + \alpha$  projection exhibits a prominent peak at the same triton energy, indicating the principal decay mode of this  $T = 2$  state.

The net number of events associated with the various  $T = 2$  decay modes was found by summing the projected spectra over the triton energy interval containing the  $T = 2$  triton peak as determined from the singles spectrum, and subtracting: 1) the "real" three-particle continuum background; and 2) the "chance" background. The former was assumed to vary linearly over the  $T = 2$  interval and, hence, was estimated by interpolating the background height on either side of this interval. The chance background was calculated from the known singles counting rates together with the known singles spectrum shapes. This method for calculating the number of chance events occurring in any region of the two-dimensional arrays was always tested by comparing its results to the observed numbers of events occurring in portions of the arrays where only chance events could contribute (for example, the regions corresponding to 24.8 MeV tritons in Fig. 2). Both kinds of background subtractions were usually small compared to the total number of events observed for dominant transitions.

The branching ratios were calculated by comparing the net number of coincidence events in a given decay mode to the number predicted from the net number of triton singles counts, the decay telescope solid angles, and the Jacobian relating laboratory cross sections to those in the coordinate system at rest with respect to the recoiling  $T = 2$  state. All the  $T = 2$  states discussed here have spin-parity  $0^+$  and decay isotropically in this coordinate system.

## RESULTS

Spectra of the projected coincidence data together with the triton singles spectra for  $^{20}\text{Ne}$  and  $^{32}\text{S}$  are shown in Figs. 5 and 6 (similar figures for  $^{24}\text{Mg}$  and  $^{28}\text{Si}$  appear in Ref. 10). The relatively poor quality  $^{20}\text{Ne}$  data is in part related to the geometry of the gas target experiment which resulted in appreciably smaller real to chance counting rate ratios compared to the solid target data. For both this reason, and the small solid angle of the single decay telescope, relatively few data were obtained. Table I summarizes the branching ratio results for all five  $T = 2$  states. The standard deviations tabulated for the individual decay modes in the table represent only counting statistics. The deviations listed for the summed branching ratios also include uncertainties in the decay telescope solid angles and an assumed 10% uncertainty in the net number of triton singles counts contained in the  $T = 2$  peaks arising from the possible presence of small peaks in the continuum background.

The summed branching ratios (X100) clearly should be less than or equal to 100%. It is apparent from the table that the sums are in fact close to 100%. Although the experimental technique used in the present work does not permit examination of all energetically-allowed decay modes because of experimental cutoffs, in general barrier penetration effects make transitions to high-lying states which could not have been detected relatively unimportant. Column five in the table lists the branching ratios after normalization to 100%—it is not implied that gamma decays or unexamined particle decays do not make small contributions to the total widths. For convenience, the decay schemes also are presented in Figs. 7 through 11 where all the states of the  $(Z-1, N)$  and  $(Z-2, N-2)$  residual nuclides lying below the  $T = 2$  states are illustrated.<sup>12</sup>

A necessary condition for events ascribed to the decay of the spin zero  $T = 2$  states is that branching ratios derived from each decay telescope be the same, since the decay is presumably isotropic. The ratios of branching ratios for all the major decay modes found from the  $-90$  degree and  $-125$  degree telescopes are listed in Table II; they lie within one standard deviation of unity and are thus consistent with this requirement.

### DISCUSSION

The  $T = 2$  states investigated in the present work are found to decay both by isospin-forbidden proton and alpha-particle emission. Moreover, excluding the  $T = 2$  state in  $^{20}\text{Ne}$ , these states have large branching ratios for decay to the ground states of the residual nuclides. This second property makes feasible the task of locating the states as compound nuclear resonances, and all have now been located utilizing this technique except the one in  $^{40}\text{Ca}$ . The resonance data have generally provided precise determinations of the excitation energies and total width upper limits, but have not been utilized to yield information about the particle-decay branching ratios; this prohibits quantitative comparisons with the results given here. [An exception is the work<sup>4,5</sup> on  $^{19}\text{F} + p$  which gives  $\Gamma_{p_0}/\Gamma = 6.2 \pm 0.4\%$  and  $\Gamma = 2.1 \pm 0.5$  keV for the  $^{20}\text{Ne}$ ,  $T = 2$  state. From Table I,  $\Gamma(p_0 + p_1 + p_2)/\Gamma \sim 14 \pm 9\%$ .] Both the observations<sup>6</sup> of the  $T = 2$  states of  $^{24}\text{Mg}$ ,  $^{28}\text{Si}$ , and  $^{32}\text{S}$  as resonances in  $^{23}\text{Na} + p$ ,  $^{24}\text{Mg} + \alpha$ , and  $^{31}\text{P} + p$  and the unsuccessful attempt<sup>13</sup> to observe the  $^{28}\text{Si}$  state as an  $^{27}\text{Al} + p$  resonance are in qualitative agreement with the present results.

Before conclusions concerning the importance of various kinds of isospin-admixtures can be made, barrier penetration factors should be

considered. Table III lists the Wigner-limit width calculated from graphs<sup>14</sup> of Coulomb wave functions. Since the widths for the two types of decay are comparable, the specific decay properties evidently are strongly influenced by the details of the admixed lower isospin configurations. The problem of interpretation is complicated because the data span the region from the  $1d_{5/2}$ ,  $2s_{1/2}$ , shells, where deformations exist, to the  $1d_{3/2}$ ,  $1f_{7/2}$  shells where the spherical shell model has some validity. A modest attempt to estimate the kinds of impurities which would be introduced by the Coulomb potential was undertaken in  $^{40}\text{Ca}$  in order to ascertain whether large  $\Delta T = 2$  admixtures (which presumably account for the alpha particle decay) might be expected.

The simple mixing calculation assumed pure shell-model configurations and included isospin mixing in only the outer (unfilled) shells. The  $T = 2$  state of  $^{40}\text{Ca}$  was taken to have the structure  $| (1d_{3/2})_{01}^{-2} (1f_{7/2})_{01}^2; 02 \rangle$ . Amplitudes of admixtures of several  $T' = 0$  or  $T' = 1$  states in this  $T = 2$  state, and also of a  $T' = 2$  state into the  $T = 0$   $^{36}\text{Ar}$  ground state were calculated in first order perturbation theory. The  $^{36}\text{Ar}$  ground state was assumed to have the structure  $| (1d_{3/2})_{00}^4; 00 \rangle$  and the alpha particle isospin impurity was ignored. The matrix elements of the Coulomb potential,  $\langle \Psi(T) | V_c | \Psi(T') \rangle$ , were calculated for these components using harmonic oscillator wave functions with a size parameter  $\nu = m\omega/\hbar = 0.25 \text{ fm}^{-2}$ . The irreducible tensor components of  $V_c$  which have rank one and two have selection rules  $\Delta T = 1$  and  $\Delta T = 2, 0$  respectively for self-conjugate nuclides. The  $T'$  states considered in  $^{40}\text{Ca}$  included the 0 particle-0 hole ground state, the 4 particle-4 hole state<sup>15</sup> at 3.35 MeV, and the 2 particle-2 hole states having the same nuclear configurations assumed for the  $T = 2$  state, but recoupled in isospin to zero or one. These last states

are the so-called anti-analog states and the Coulomb matrix elements were expected to be relatively large. The locations of these states are not established experimentally; however, in the  $^{40}\text{K}$  energy level scheme,<sup>12</sup> the lowest spin zero state appears to lie no lower than 2.3 MeV. Assuming that this is the location of the  $T = T_z = 1, 2$  particle-2 hole state, then its analog in  $^{40}\text{Ca}$  lies at about 10 MeV. Since the energy splitting between analog and anti-analog states is thought to be proportional to  $\vec{T}_1 \cdot \vec{T}_2$  (see Refs. 16 17), the  $(T = 0)2$  particle-2 hole state is therefore expected to lie at about 9 MeV.

The calculated admixture coefficients  $\alpha_{TT'} = \{\langle \Psi(T) | V_c | \Psi(T') \rangle / (E_{T'} - E_T)\}$  are tabulated in Table IV; note that the largest coefficient occurs for the  $T' = 1$  anti-analog state. Only a few  $T'$  states were considered and, of course, many other states exist near the  $T = 2$  state at 11.98 MeV. Nevertheless, within the framework of this initial calculation it is perhaps reasonable to ignore most of these other states since only a small fraction of these states will have zero angular momentum and none are expected to have the structure required to produce large Coulomb matrix elements. [The latter speculation is clearly true only to the extent that the  $T = 2$  state consists solely of the assumed 2 particle-2 hole configuration.] The admixtures listed in the table do not appear to be large enough to yield a  $\Delta T = 2$  decay width of, say, 1 keV. It would be useful to have accurate width measurements from resonance experiments; however, it appears unlikely on the basis of known widths for similar analog states that the type of mixing considered here would be able to account for it.

On the basis of the calculated admixtures,  $\ell = 3$  proton emission to a low-lying  $J^\pi = 7/2^-$  state of  $^{39}\text{K}$  resulting from the rather large  $\Delta T = 1$ ,

2 particle-2 hole admixture might be expected rather than alpha particle decay. Unfortunately, the small penetration factor for decay to the  $^{39}\text{K}$  2.82-MeV state effectively precludes this mode of decay, preventing examination of the importance of this admixture. Generalizing these speculations, i.e., that mixing with the anti-analog states might influence the decay properties of  $T = 2$  states in the other nuclei that were examined, it turns out that in every case either small penetration factors or small overlaps of initial and final states (assuming for simplicity that the  $T = 2$  analog states in the lighter nuclides have structures given by the axially symmetric Nilsson model) may hinder proton emission. Thus, the absence of any proton decay to excited states in the  $(Z-1, N)$  residual nuclides does not reflect upon the importance of such mixing. It is clear, however, that neither the observed ground state proton decay of  $^{24}\text{Mg}$  or  $^{32}\text{S}$  nor the alpha particle decay of the other  $T = 2$  states can be adequately explained by the methods used.

Many aspects of the isospin mixing problem have not been considered: the states undoubtedly have more complicated structure than is considered here and the calculational approach used is actually only appropriate for calculating impurities in low-lying bound states, i.e., the "external" mixing arising from the different neutron and proton wave functions in the exterior region is completely ignored.<sup>18</sup>

It is hoped that the experimental results presented here will stimulate more extensive theoretical efforts to describe the isospin-forbidden decay properties of these states. In particular, it will be interesting to learn whether the Coulomb potential is capable of generating the  $\Delta T = 2$  admixtures implied by the observed alpha particle decay of several of the states which have been studied.



FOOTNOTES AND REFERENCES

<sup>†</sup>This work performed under the auspices of the U. S. Atomic Energy Commission.

1. W. H. MacDonald, Nuclear Spectroscopy, Part B, ed. by F. Ajzenberg-Selove, (Academic Press, New York, 1960) p. 932.
2. D. H. Wilkinson, ibid, p. 852.
3. R. J. Blin-Stoyle, Selected Topics in Nuclear Spectroscopy, ed. by B. J. Verhaar, (North-Holland Publishing Co., Amsterdam, 1964) p. 213.
4. R. Bloch, R. E. Pixley, and P. Truöl, Phys. Letters 25B, 215 (1967).
5. H. M. Kuan, D. W. Heikkinen, K. A. Snover, F. Riess, and S. S. Hanna, Phys. Letters 25B, 217 (1967).
6. F. Riess, W. J. O'Connell, D. W. Heikkinen, H. M. Kuan, and S. S. Hanna, Phys. Rev. Letters 19, 367 (1967); K. A. Snover, D. W. Heikkinen, F. Riess, H. M. Kuan, and S. S. Hanna, Phys. Rev. Letters 22, 239 (1969); D. W. Heikkinen, H. M. Kuan, K. A. Snover, F. Riess, and S. S. Hanna, Bull. Am. Phys. Soc. 13, 884 (1968).
7. J. Cerny, Annual Reviews of Nuclear Science, Vol. 18, ed. by E. Segrè, (Annual Reviews Inc., Palo Alto, California, 1968) p. 27.
8. D. J. Bredin, O. Hansen, G. M. Temmer, and R. Van Bree, Isobaric Spin in Nuclear Physics, ed. by J. D. Fox and D. Robson, (Academic Press, Inc., New York, 1966) p. 472. G. M. Temmer and R. Van Bree, International Nuclear Physics Conference, Gatlinburg, Tennessee, ed. by R. L. Becker, C. D. Goodman, P. H. Stelson, and A. Zucker, (Academic Press, Inc., New York, 1967) p. 885.
9. G. M. Temmer, Proc. Int. Conf. on Nuclear Structure, Dubna, (International Atomic Energy Agency, Vienna, 1968) p. 249.

10. R. L. McGrath, S. W. Cospers, and J. Cerny, Phys. Rev. Letters 18, 243 (1967)  
R. L. McGrath, J. C. Hardy, and J. Cerny, Phys. Letters 27B, 443 (1968).  
Within experimental uncertainties, these preliminary data agree with the present results.
11. S. W. Cospers, H. Brunnader, J. Cerny, and R. L. McGrath, Phys. Letters 25B, 324 (1967).
12. T. Lauritsen and F. Ajzenberg-Selove, Nuclear Data Sheets, compiled by K. Way et al., (Printing and Publishing Office, National Academy of Sciences - National Research Council, Washington, D. C., 1962); P. M. Endt and C. Van der Leun, Nucl. Phys. A105, 1 (1967). The  $^{23}\text{Na}$  level scheme is taken from A. R. Poletti and D. F. H. Start, Phys. Rev. 147, 800 (1966), and references therein.
13. H. M. Kuan, F. Riess, K. A. Snover, D. W. Heikkinen, D. C. Healey, and S. S. Hanna, Bull. Am. Phys. Soc. 13, 884 (1968).
14. W. T. Sharp, H. E. Gove, and E. B. Paul, Atomic Energy of Canada Limited Report No. 268, 1955 (unpublished).
15. J. R. MacDonald, D. F. H. Start, R. Anderson, A. G. Robertson, and M. A. Grace, Nucl. Phys. A108, 6 (1968); W. J. Gerace and A. M. Green, Nucl. Phys. 93, 110 (1967).
16. R. K. Bansal and J. B. French, Phys. Letters 11, 145 (1964).
17. L. Zamick, Phys. Letters 19, 580 (1965).
18. D. Robson, Annual Review of Nuclear Science, Vol. 16, ed. by E. Segrè, (Annual Reviews, Inc., Palo Alto, California, 1966) p. 119.

Table I. Summary of T = 2 branching ratio data.

Mode	Net events	Branching <sup>a</sup> ratios (X100)	Summed <sup>b</sup> branching ratios	Normalized branching ratios
$^{20}\text{Ne} \rightarrow ^{16}\text{O} + \alpha_0$	-3±2	-6±5		~0
$^{16}\text{O} + (\alpha_1 + \alpha_2)$	17±6	35±12		38
$^{16}\text{O} + (\alpha_3 + \alpha_4)$	15±6	29±12		32
$^{19}\text{F} + (p_0 + p_1 + p_2)$	7±4	14±9		16
$^{19}\text{F} + (p_3 + p_4 + p_5)$	6±4	13±8		14
			85±29	
$^{24}\text{Mg} \rightarrow ^{23}\text{Na} + p_0$	108±11	71±7		74
$^{23}\text{Na} + p_1$	1±6	1±4		1
$^{20}\text{Ne} + \alpha_0$	7±6	3±3		3
$^{20}\text{Ne} + \alpha_1$	48±10	22±4		22
			97±16	
$^{28}\text{Si} \rightarrow ^{24}\text{Mg} + \alpha_0$	93±10	72±8		81
$^{24}\text{Mg} + \alpha_1$	11±5	8±4		9
$^{27}\text{Al} + p_0$	4±7	4±8		5
$^{27}\text{Al} + (p_1 + p_2)$	4±5	4±5		5
			88±16	
$^{32}\text{S} \rightarrow ^{31}\text{P} + p_0$	32±6	86±17		75
$^{28}\text{Si} + \alpha_0$	9±4	18±7		16
$^{28}\text{Si} + \alpha_1$	6±3	11±5		9
			115±24	

(continued)

Table I. Continued.

Mode	Net events	Branching <sup>a</sup> ratios (X100)	Summed <sup>b</sup> branching ratios	Normalized branching ratios
$^{40}\text{Ca} \rightarrow ^{36}\text{Ar} + \alpha_0$	125±12	116±11		100
$^{36}\text{Ar} + \alpha_1$	-2±2	-1±2		~0
$^{39}\text{K} + p_0$	-2±7	-3±9		~0
			112±19	

<sup>a</sup>Standard deviation includes only counting statistics.

<sup>b</sup>Standard deviation also includes uncertainties in the number of triton counts and in decay telescope solid angles as explained in the text.

Table II. Ratios of branching ratios derived from delay telescope data at  $-90$  degrees compared to telescope data at  $-125$  degrees.

Decay mode	Ratio: $\frac{\text{Branching ratio } (-90^\circ)}{\text{Branching ratio } (-125^\circ)}$
$^{24}\text{Mg} \longrightarrow ^{23}\text{Na} + p_0$	$1.24 \pm 0.28$
$^{24}\text{Mg} \longrightarrow ^{20}\text{Ne} + \alpha_1$	$1.50 \pm 0.59$
$^{28}\text{Si} \longrightarrow ^{24}\text{Mg} + \alpha_0$	$1.08 \pm 0.23$
$^{32}\text{S} \longrightarrow ^{31}\text{P} + p_0$	$0.86 \pm 0.35$
$^{40}\text{Ca} \longrightarrow ^{36}\text{Ar} + \alpha_0$	$1.28 \pm 0.26$

Table III. Wigner-limit widths for particle decay of  $T = 2$  states  
 where  $\Gamma = 3 \cdot R / (F_l^2 + G_l^2) \cdot \hbar^2 / MR$ .

$T = 2$ state	$\Gamma_{p_0}^a$	$l_{p_0}$	$\Gamma_{\alpha_0}^b$
$^{20}\text{Ne}$	7.25 MeV	s	7.85 MeV
$^{24}\text{Mg}$	1.41	d	3.11
$^{28}\text{Si}$	0.66	d	1.29
$^{32}\text{S}$	2.70	s	0.65
$^{40}\text{Ca}$	0.38	d	0.13

$$^a R = 1.5 A^{1/3} \text{ fm.}$$

$$^b R = (1.4 A^{1/3} + 1.6) \text{ fm.}$$

Table IV. Calculated isospin admixtures  $\alpha_{TT'}$  in the  $^{40}\text{Ca}$   
 $T = 2$  state and  $^{36}\text{Ar}$  ground state.

	Excitation	$\langle T=2   V_c   T' \rangle$	$\alpha_{TT'}$
<u><math>^{40}\text{Ca}</math></u>			
$ (1d_{3/2})^{-2} (1f_{7/2})^2 J=0, T=2\rangle$			
→ $ (1d_{3/2})^8 T'=0\rangle$	0.0 MeV	16 MeV	$1.3 \times 10^{-3}$
→ $ (1d_{3/2})^{-4} (1f_{7/2})^4 T'=0\rangle$	3.35	13	$1.5 \times 10^{-3}$
→ $ (1d_{3/2})^{-2} (1f_{7/2})^2 T'=0\rangle$	$\sim 9$	22	$7.3 \times 10^{-3}$
→ $ (1d_{3/2})^{-2} (1f_{7/2})^2 T'=1\rangle$	$\sim 10$	420	$2.1 \times 10^{-1}$
<u><math>^{36}\text{Ar}</math></u>			
$ (1d_{3/2})^4 J=0, T=0\rangle$			
→ $ (1d_{3/2})^4 T'=2\rangle$	10.86	150	$1.4 \times 10^{-2}$

The size parameter is  $v = 0.25 \text{ fm}^{-2}$ .

## FIGURE CAPTIONS

Fig. 1. A schematic diagram of the experimental apparatus. Telescope #1 detected tritons, and "decay" telescopes #2 and #3 detected either protons or particles stopping in the  $\Delta E$  detectors (alpha particles). If one of these events arrived in coincidence with a triton, the appropriate linear and logic signals were passed on to the multiplexer—A.D.C. and to the computer. [The electronics for telescope #2 are similar to #3 and are not shown.]

Fig. 2. A two-dimensional energy spectrum of triton-proton coincidence events from the  $^{42}\text{Ca}(p,t)^{40}\text{Ca} \rightarrow p + ^{39}\text{K}$  reaction. The diagonal lines labeled by the residual states of  $^{39}\text{K}$  were calculated from the kinematics.

Fig. 3. A two-dimensional energy spectrum of events consisting of tritons in coincidence with particles which stopped in the  $\Delta E$  detector of telescope #3. From the  $\Delta E$  energy losses, these particles are known to be alpha particles and, consequently, the data correspond to the  $^{42}\text{Ca}(p,t)^{40}\text{Ca} \rightarrow \alpha + ^{36}\text{Ar}$  reaction. As in Fig. 2, the diagonal lines were calculated from the kinematics. The cluster of events along the  $^{36}\text{Ar}$  ground state line at 22.4 MeV triton energy is associated with the decay of the  $0^+ T = 2$  state located at 11.98 MeV in  $^{40}\text{Ca}$ .

Fig. 4. The top spectrum shows the triton singles data containing the  $^{40}\text{Ca}$   $T = 2$  state. The lower-lying excited states are not observed because of the relatively thin detectors used in the triton telescope. The lower spectra are summed projections from both decay telescopes of events lying along kinematic bands in the coincidence data onto the triton energy axis; the arrows in these spectra mark the energy cutoffs determined by kinematics and detector thicknesses.



Fig. 5. The top spectrum shows some of the triton singles data from the  $^{22}\text{Ne}(p,t)^{20}\text{Ne}$  reaction; the projected coincidence data are shown in the lower spectra. The events in the interval between the arrows drawn on either side of the  $T = 2$  state peak were summed to obtain the branching ratios.

Fig. 6. Triton singles data containing the  $0^+ T = 2$  state in  $^{32}\text{S}$ , together with the summed projections of the coincidence data (see Fig. 4 caption).

Fig. 7. Decay scheme showing energetically-allowed particle-decay models of the 16.73 MeV  $T = 2$  state of  $^{20}\text{Ne}$ . The level data are taken from the literature. The normalized branching ratios determined in this work are given alongside the arrows.

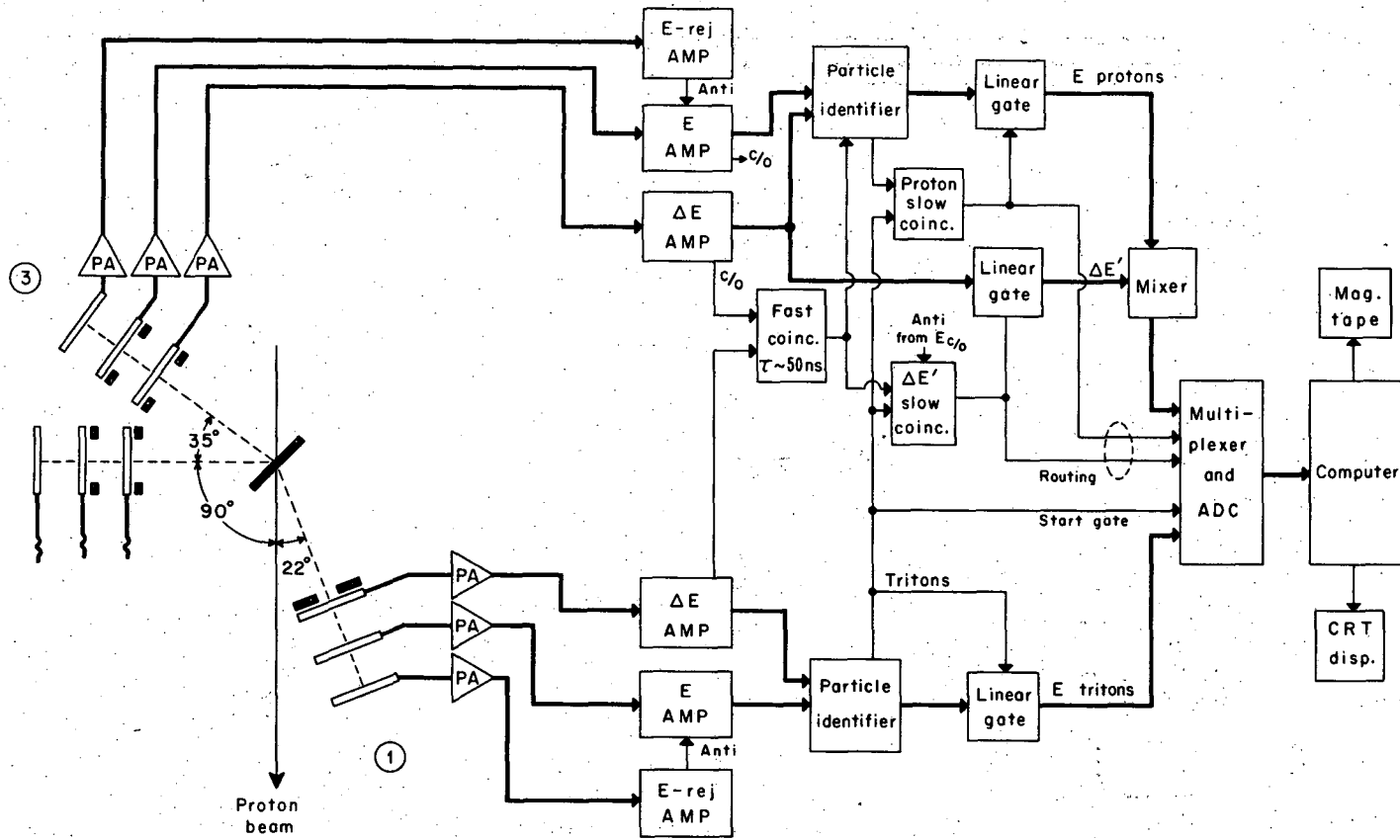
Fig. 8. Decay scheme for the 15.43 MeV  $T = 2$  state of  $^{24}\text{Mg}$ . (See Fig. 7 caption).

Fig. 9. Decay scheme for the 15.21 MeV  $T = 2$  state of  $^{28}\text{Si}$ . (See Fig. 7 caption).

Fig. 10. Decay scheme for the 11.98 MeV  $T = 2$  state of  $^{32}\text{S}$ . (See Fig. 7 caption).

Fig. 11. Decay scheme for the 11.98 MeV  $T = 2$  state of  $^{40}\text{Ca}$ . (See Fig. 7 caption).

FIG. 1



XBL687-3282

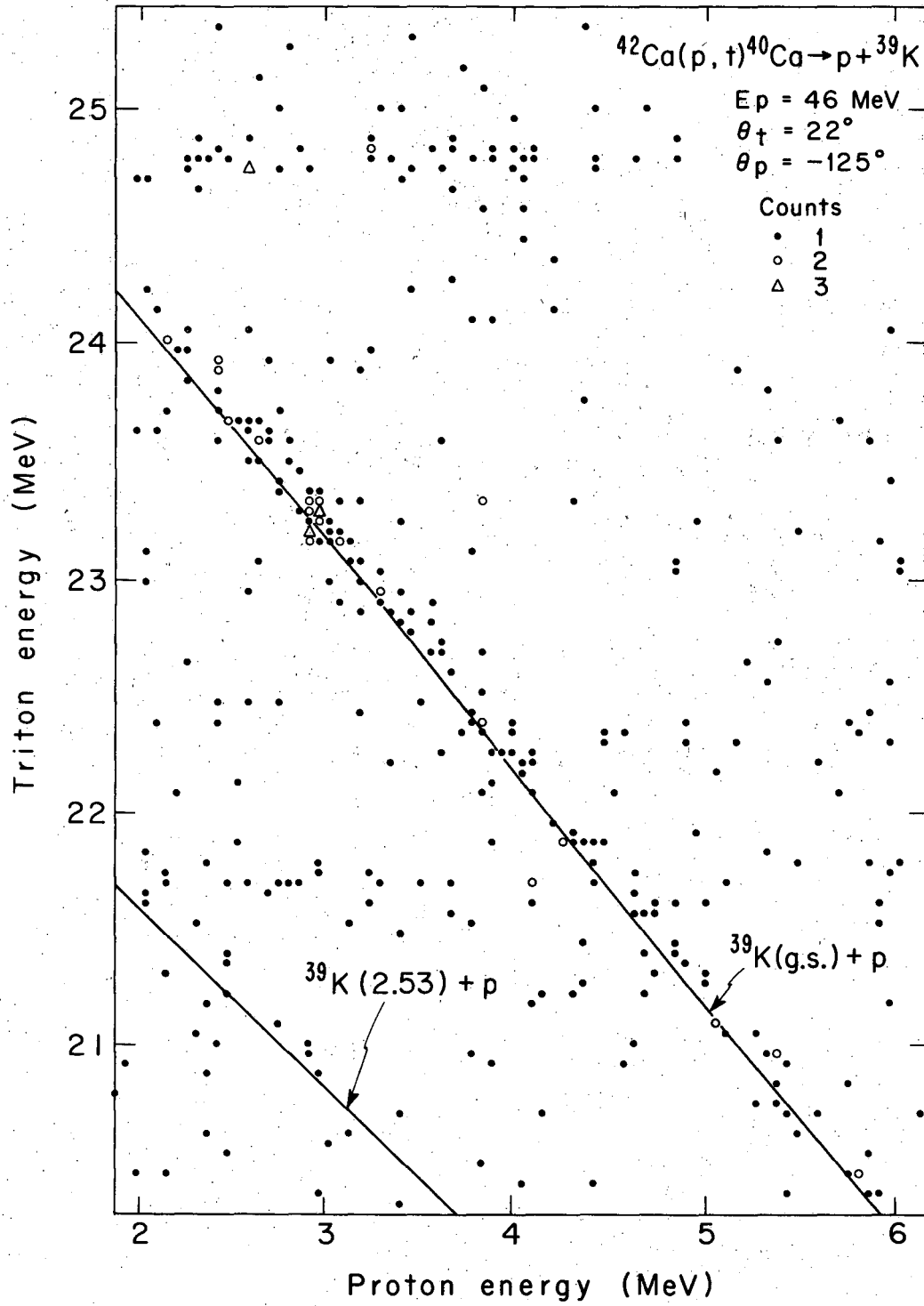
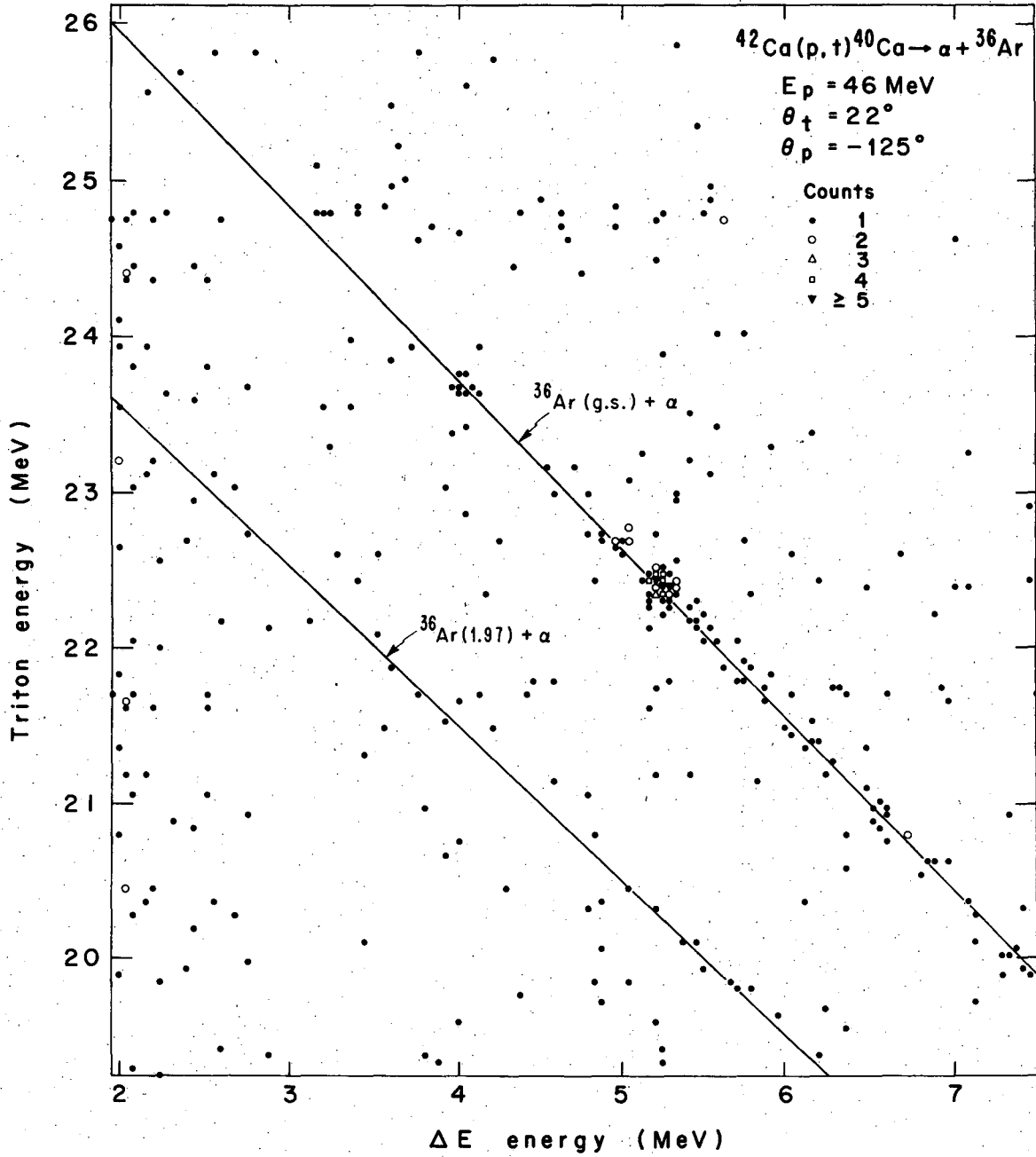


Fig. 2

XBL 687-3278



XBL687-3281

Fig. 3

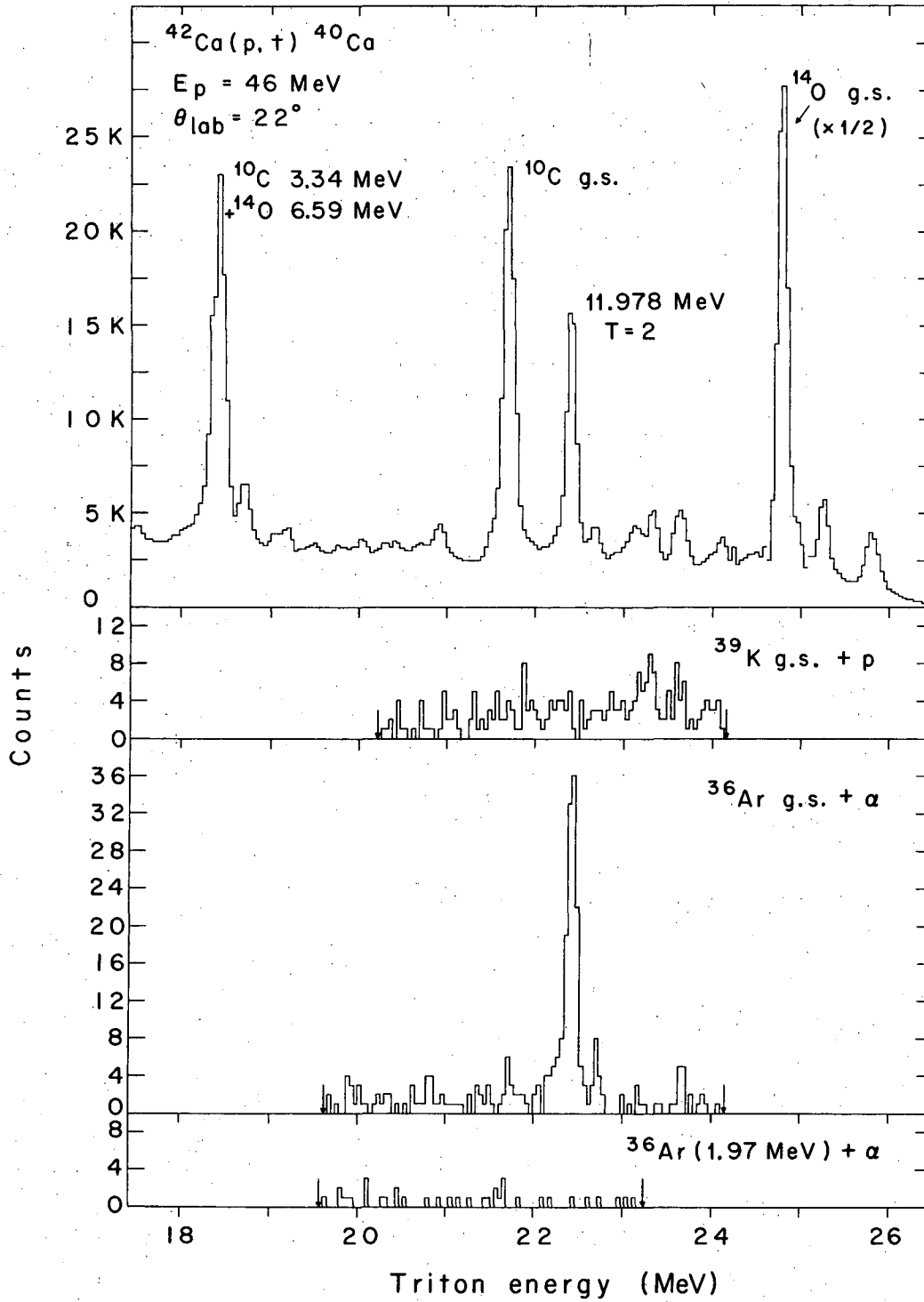


Fig. 4

XBL687-3279

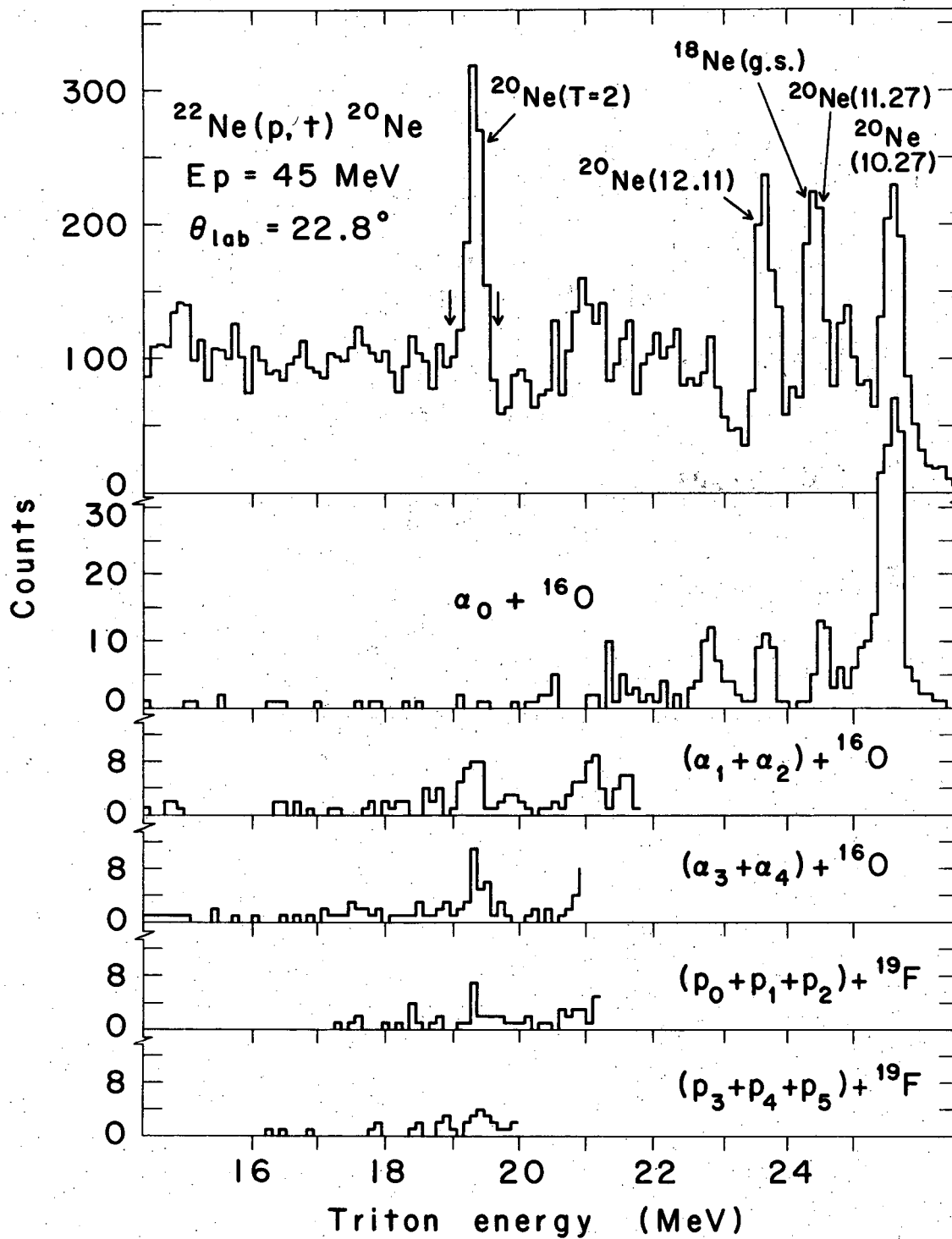


Fig. 5

XBL6711-5606

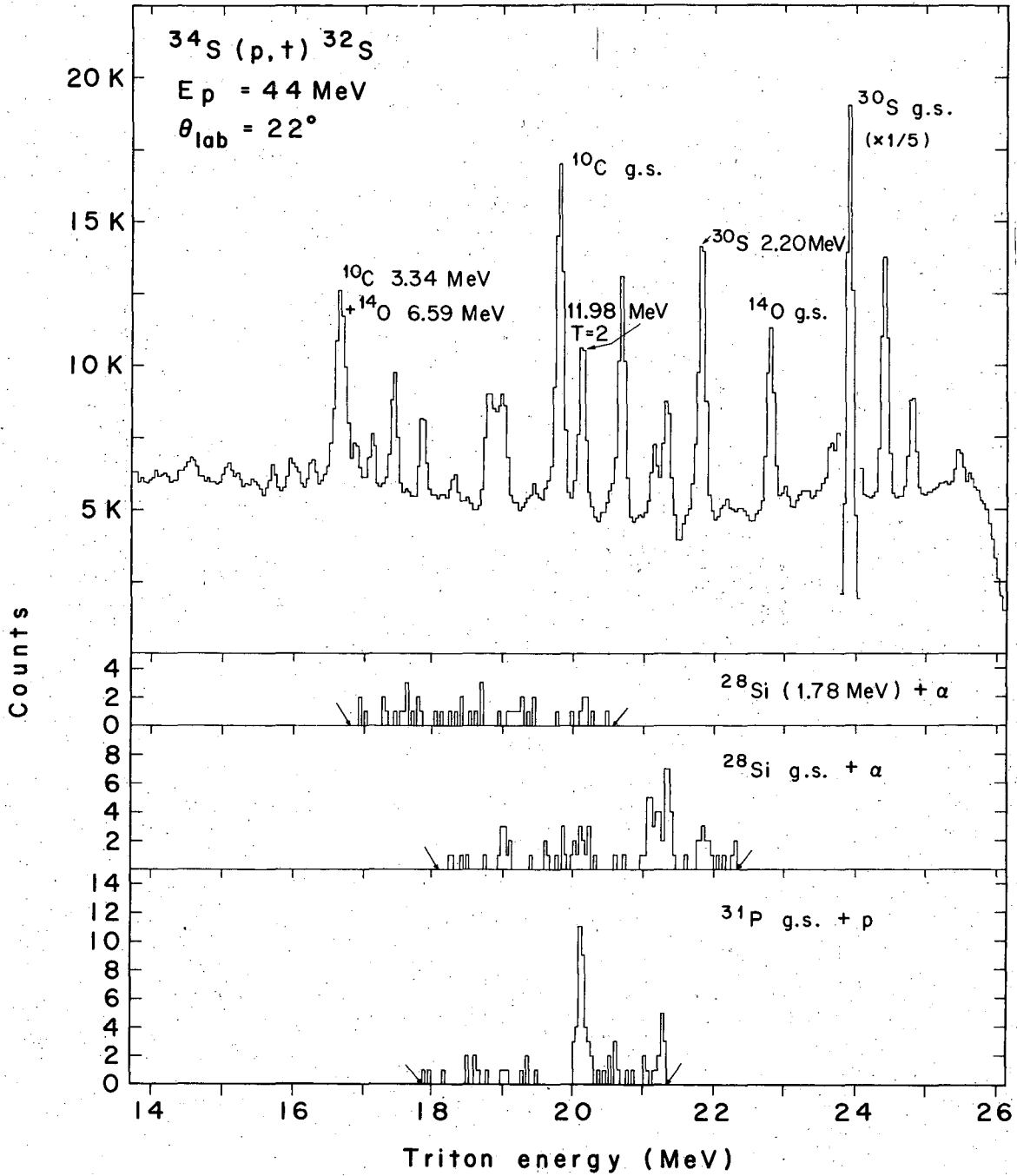
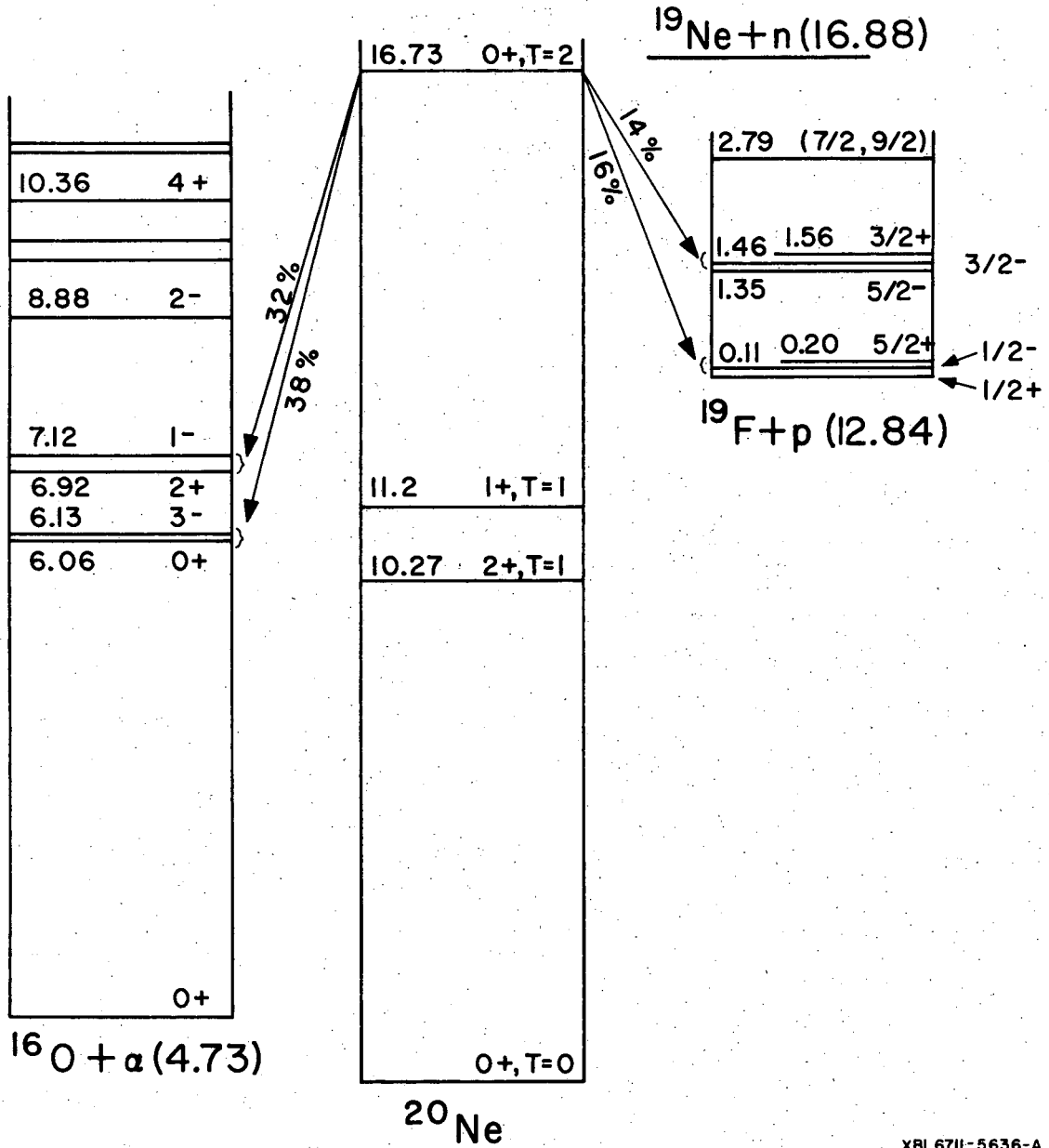


Fig. 6



XBL6711-5636-A

Fig. 7



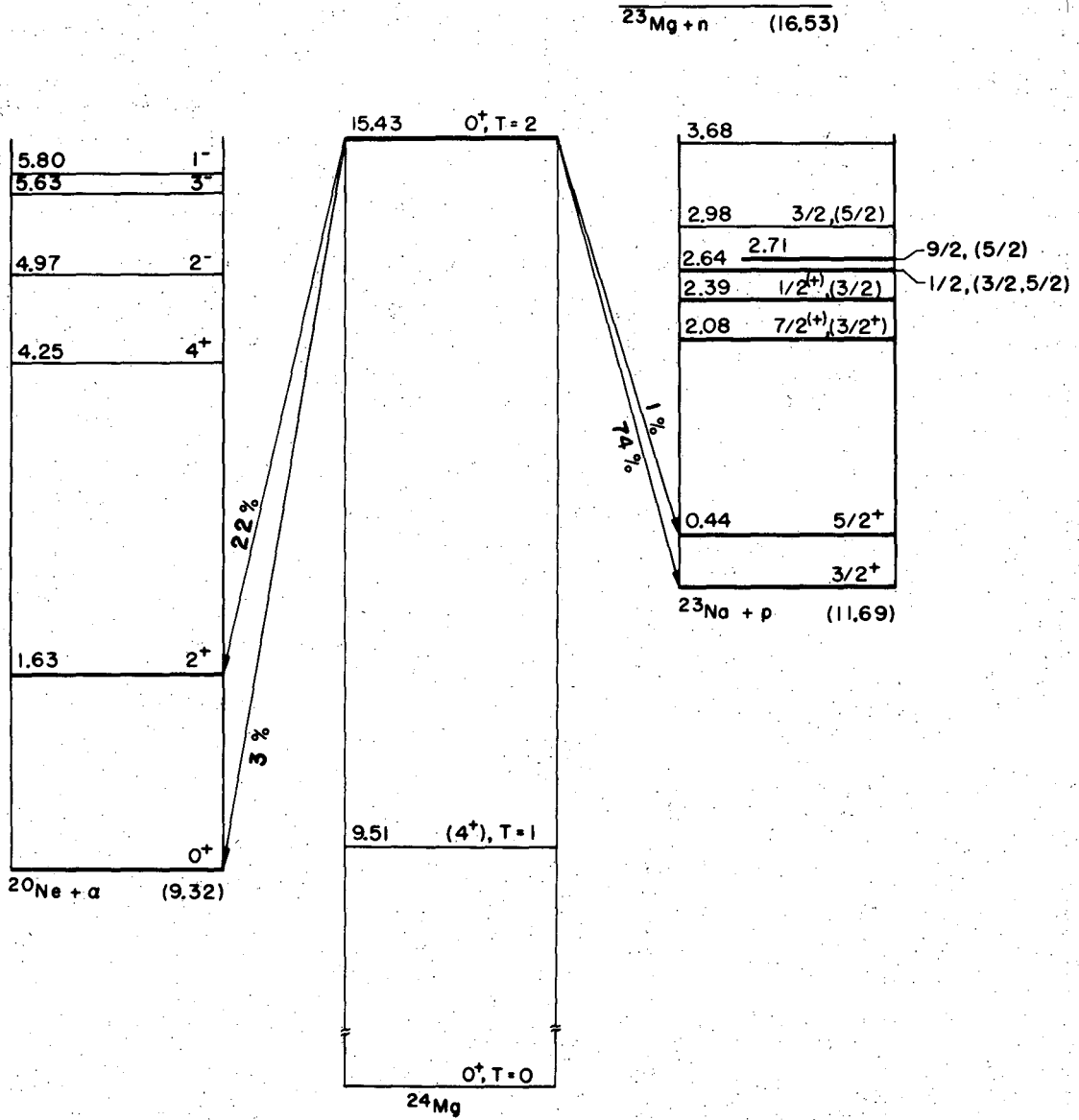
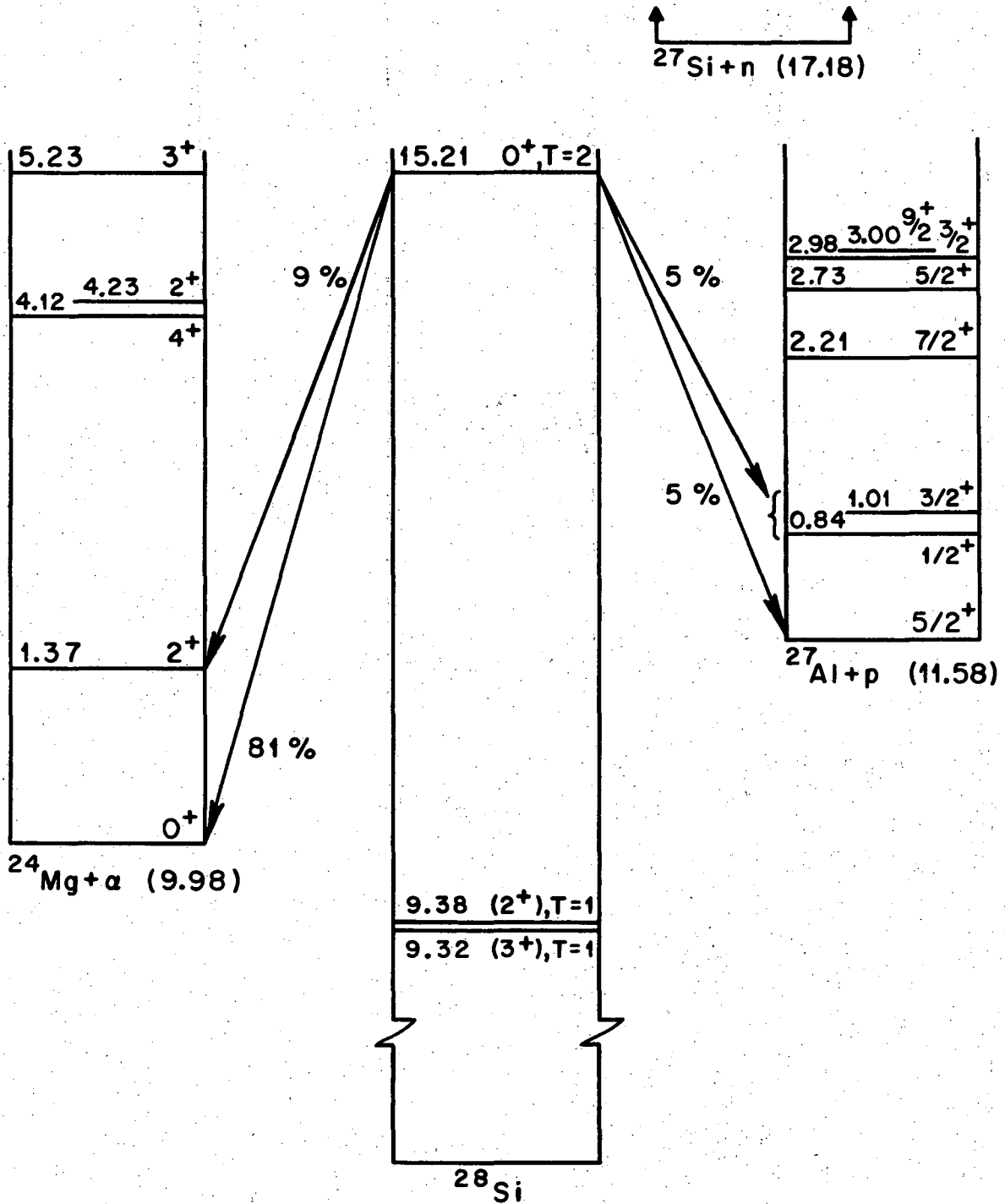
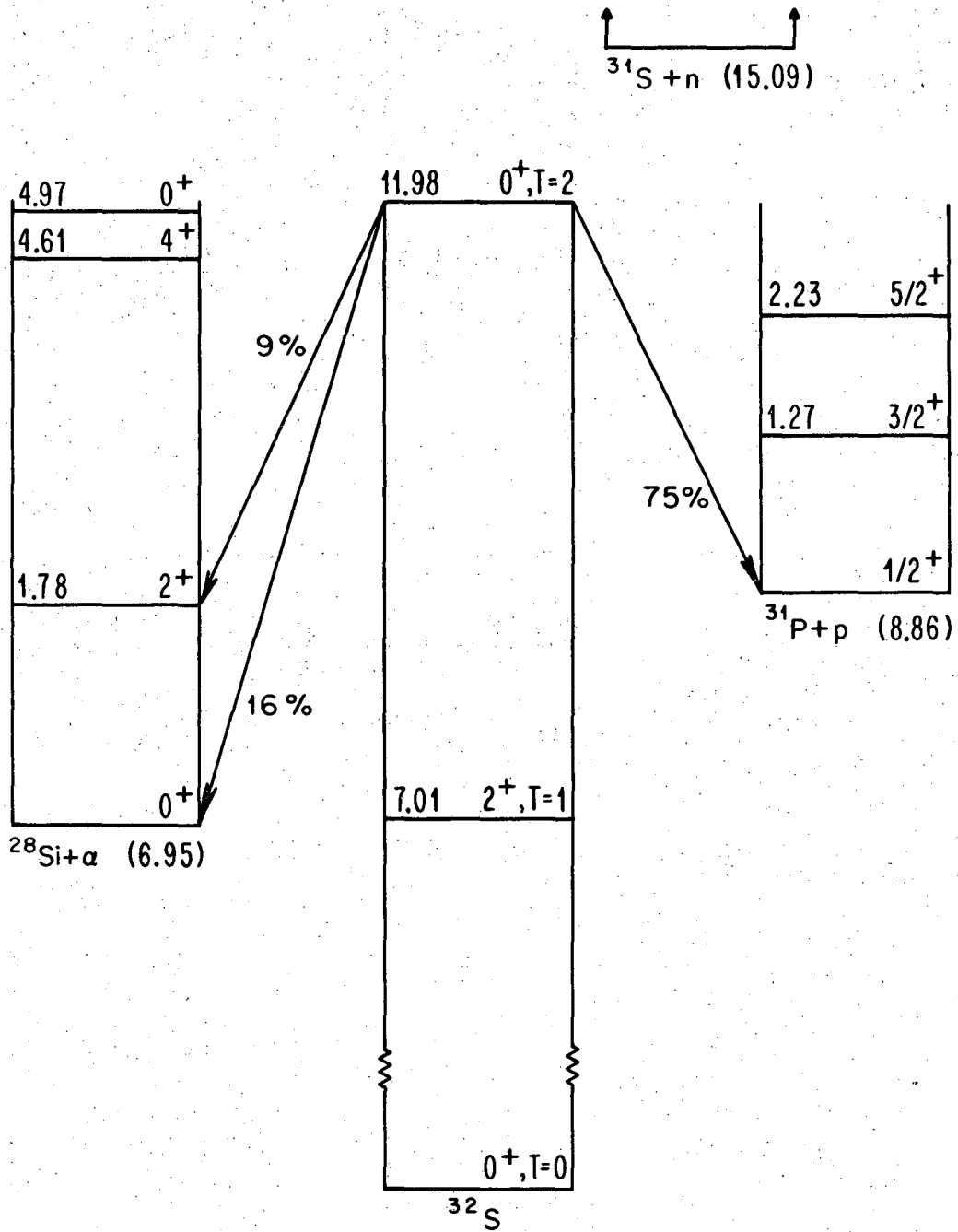


Fig. 8



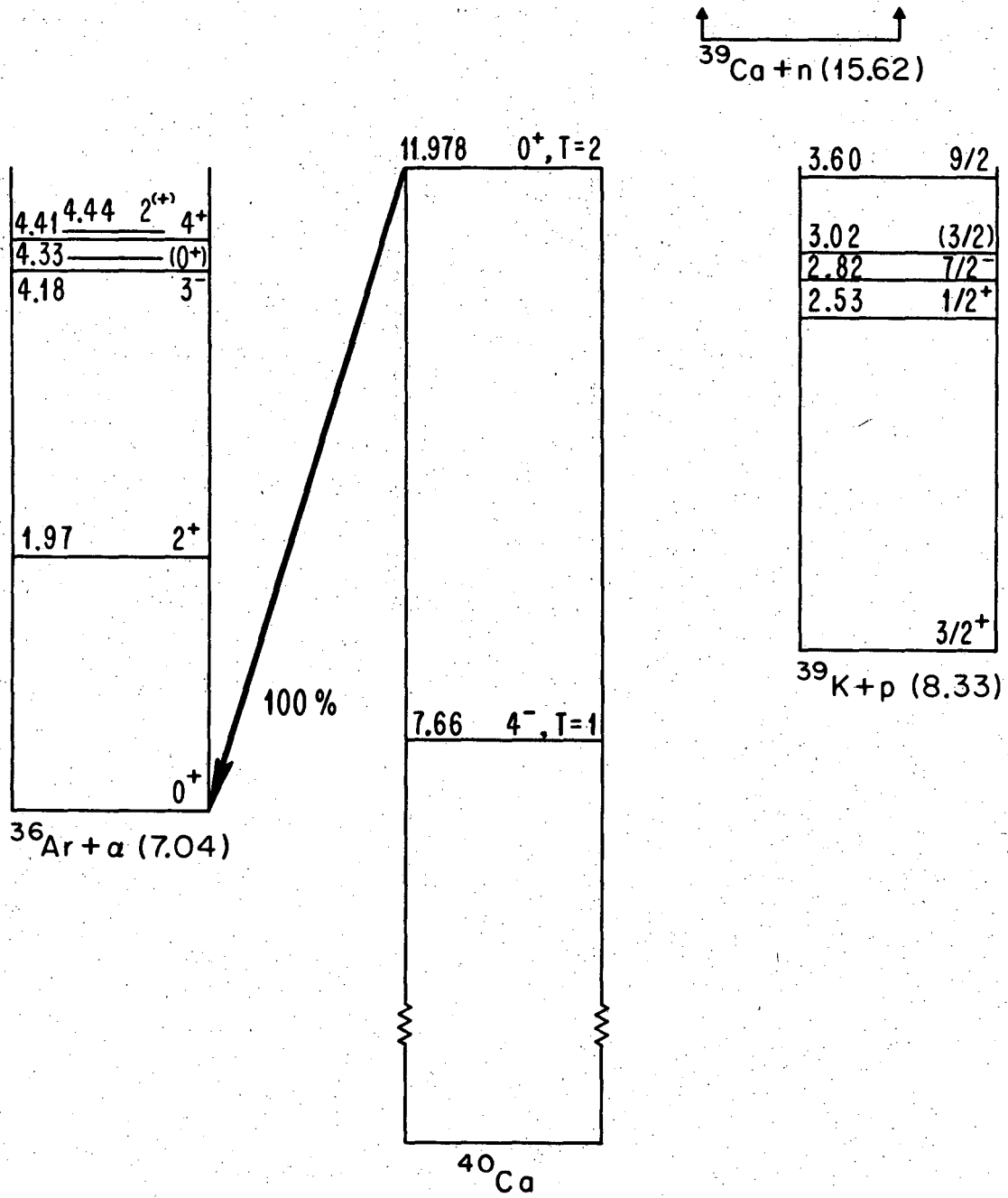
XBL 686-3074

Fig. 9



XBL688-3518

Fig. 10



XBL687-3280

Fig. 11

LEGAL NOTICE

*This report was prepared as an account of Government sponsored work. Neither the United States, nor the Commission, nor any person acting on behalf of the Commission:*

- A. Makes any warranty or representation, expressed or implied, with respect to the accuracy, completeness, or usefulness of the information contained in this report, or that the use of any information, apparatus, method, or process disclosed in this report may not infringe privately owned rights; or*
- B. Assumes any liabilities with respect to the use of, or for damages resulting from the use of any information, apparatus, method, or process disclosed in this report.*

*As used in the above, "person acting on behalf of the Commission" includes any employee or contractor of the Commission, or employee of such contractor, to the extent that such employee or contractor of the Commission, or employee of such contractor prepares, disseminates, or provides access to, any information pursuant to his employment or contract with the Commission, or his employment with such contractor.*

TECHNICAL INFORMATION DIVISION  
LAWRENCE RADIATION LABORATORY  
UNIVERSITY OF CALIFORNIA  
BERKELEY, CALIFORNIA 94720